Some results of Schumann resonance studies at a low latitude station Agra, India during post period of solar cycle minimum 2008-2009

Birbal Singh[$,*] & Devbrat Pundhir

Department of Electronics and Communication Engineering, RBS Engineering Technical Campus, Bichpuri, Agra 283 105, India
[$]E-mail: bbsagra@gmail.com

The characteristics of Schumann resonance (SR) have been studied at a low latitude station Agra (geographic latitude 27.2°N, longitude 78°E), India and the results obtained during two periods (01 April 2007 - 31 March 2008 and 01 March 2011 - 29 February 2012) corresponding to pre and post period of solar cycle minimum (SCM) of 2008-2009 are compared. The results show that (i) there is a shift in the peak thunderstorm activity from the month of July in the pre-SCM to August in post-SCM; (ii) the first mode frequency increases with the increasing SCM; and (iii) there are distinct drops in the frequency range dF1 in the months of August and December 2012 corresponding to effective lightning areas during the post-SCM. The seasonal variation of first mode SR frequency shows that it is theoretically dependent on source-observer distance.

Keywords: Schumann resonance, Thunderstorm activity, Lightning

PACS Nos: 92.60.Pw; 92.60.Qx; 94.20.Vv

1 Introduction

The frequency-time spectrograms of naturally occurring ultra low frequency (ULF) / extremely low frequency (ELF) electromagnetic emissions recorded carefully in a noise-free area and processed thoroughly using an advanced processing technique show intense bands at the frequencies of 8, 14, 21, …….Hz which are known as Schumann resonance (SR) modes. These are produced as a result of interaction between direct and round-the-globe ELF waves (frequency between 3 and 30 Hz) radiated from lightning discharges and propagated through the earth-ionosphere cavity. The SR phenomenon was first predicted by Schumann[1] and experimentally verified by Balser & Wagner[2]. The studies of SR have attracted greater attention rather recently due to its wide ranging applications in the fields of global thunderstorm activities, ground surface temperature, lower ionospheric dynamics during normal and perturbed days, forecast of monsoon, etc. A detailed description of the initial work done in this field based on experimental observations and theoretical treatments is given in an excellent monograph produced by Nickolaenko & Hayakawa[3]. Some very interesting recent studies related with morphology and varying geophysical conditions are given by a number of researchers[4-12].

In one of the recent papers[13], the characteristics of global thunderstorm activities extracted from SR data obtained at a low latitude station Agra (geographic latitude 27.2°N, longitude 78°E) have been studied for a period of one year during 01 April 2007 - 31 March 2008, which corresponds to pre-solar cycle minimum (SCM) of 2008-2009. In that paper, the diurnal and seasonal variations of SR intensity have been studied and compared with Optical Transient Detector (OTD) data from space, diurnal variation of first mode frequency and monthly variation of frequency range, etc. In the present paper, this work is modified and extended for a period of 12 months during 01 March 2011 - 29 February 2012, which corresponds to the post period of solar cycle minimum (SCM) of 2008-2009. Significant changes in the characteristics of SR phenomenon are found, which show a shift in global thunderstorm activities and effective lightning areas, increasing solar cycle effect on the first mode SR frequency, etc. It is also shown theoretically that diurnal variation in first mode frequency is due to variation in source-observer distance.

2 Experimental set up and Method of data processing

The details of experimental set up and method of data processing are presented in earlier paper[14]. Here, the details are mentioned briefly.

A 3-component search coil magnetometer (LEMI-30) is used, which has been procured from Lviv Center of Institute of Space Research, Ukraine. The search coils are buried underground in a relatively noise free area in agriculture fields of the Bichpuri campus of RBS College, Agra, which is located 12 km west of Agra city in rural area. The three sensors are oriented in geographical North-South (X-component), East-West (Y-component), and vertical (Z-component) directions and specifications of each of them are given in Table 1.

The LEMI-30 system has sampling rate of 256 Hz and sends these samples to dedicated PC. The LEMI-30i software in the PC takes average of each four samples simply by summing and dividing so that a binary file containing data at the sampling rate of 64 Hz is stored in the PC. The recorded data on PC in amplitude-time may be seen in frequency-time (dynamic spectra) by performing spectral analysis using FFT available in MATLAB with 1024 words of data length (temporal resolution = 16 sec, frequency resolution = 0.06 Hz) at a time. The power spectral density (PSD) of the input signal is evaluated using Welch spectral technique[15], which uses averaged modified periodograms. The PSD are prepared for each one hour data (230400 data points) and a Hamming window of 1024 data points with sliding of half the window is used to compute the modified periodogram of each segment. In this method, the spectrum obtained per hour is the average of 450 spectra with 1024 data points. The Welch method is closely related to the method of complex demodulation described by Bingham et al.[16] and hence, a separate method to extract SR model frequencies in the analysis of data is not applied. An example of dynamic spectrum and corresponding PSD obtained from the data recorded by the X-component of the sensors on 18 February 2012 is

presented in Fig. 1(a and b). As it may be seen from Fig. 1(a), four intense bands appear around the SR frequency modes (8, 14, 20, 26 Hz) and corresponding amplitudes may be determined from PSD of Fig. 1(b). The PSD shows amplitude in dB, which is converted in intensity (in nT^2 Hz^{-1}) and the results corresponding to Fig. 1(b) are shown in Fig. 1(c). In Fig. 1(a), the time is shown in hrs UT which is related with local time, LT = UT+5.5. The dynamic spectrum shows the color-coded power as a function of frequency at different time. The PSD shows the variation of amplitude in dB which has the reference level of magnetic noise levels of the sensor at different frequencies as mentioned. For example, from Fig. 1(a), -45 dB of SR frequency at 8 Hz corresponds to an amplitude of 5.6×10^{-3} nT $Hz^{-1/2}$ at the reference level of 0.03×10^{-3} nT $Hz^{-1/2}$, which is the magnetic noise level of the sensor at 8 Hz as obtained from graphical variation in the LEMI-30 manual. The corresponding intensity is the square of amplitude, which is 3.136×10^{-5} nT^2 Hz^{-1}.

Here, it may be noted that Fig. 1(a) resembles in many respect with Fig. 1(a) of Tyagi et al.[13], especially the distribution of spikes in the coloured figure. However, these two figures are different because they were observed on different days, and the differences are indicated by PSDs also. Since, the time of measurement is same during which a passenger train passes every day, similar spikes appear in both the figures. The detailed examination of the quality of the SR data shows that due to local noises including the movement of trains on a railway track (about 300 m away in East-West direction), the X-component is affected least, the Y-component moderately, but the Z-component severely. Hence, X-component data is used mostly in the present analysis. However, Y-component data is also used wherever necessary by applying careful selection of the data.

In order to further process the data, a program is written in MATLAB to extract hourly information about the peak frequencies and intensities of three modes and arrange them in separate columns in EXCEL. In this way, a time series is prepared for the frequencies and intensities of the SR data for 24 hours each day and then for 12 months from 01 March 2011 to 29 February 2012. This time series is used to deduce various characteristics of SR phenomenon observed at Agra station, some of which are described here.

Table 1 – Specifications of sensor

Dimensions	
Length	870 mm
Diameter	85 mm
Frequency range	0.001-30 Hz
Measuring range	$\pm$ 200 nT
Transformation factor	
0.001-1 Hz	$20 \times f$ mV $(nT)^{-1}$
1-30 Hz	20 mV $(nT)^{-1}$
Auxiliary output gain	20 dB
Magnetic noise level at 0.01-10 Hz	$\leq$ 20pT $Hz^{-1/2}$- $\leq$ 0.04 pT $Hz^{-1/2}$
Mains interference rejection	> 60 dB
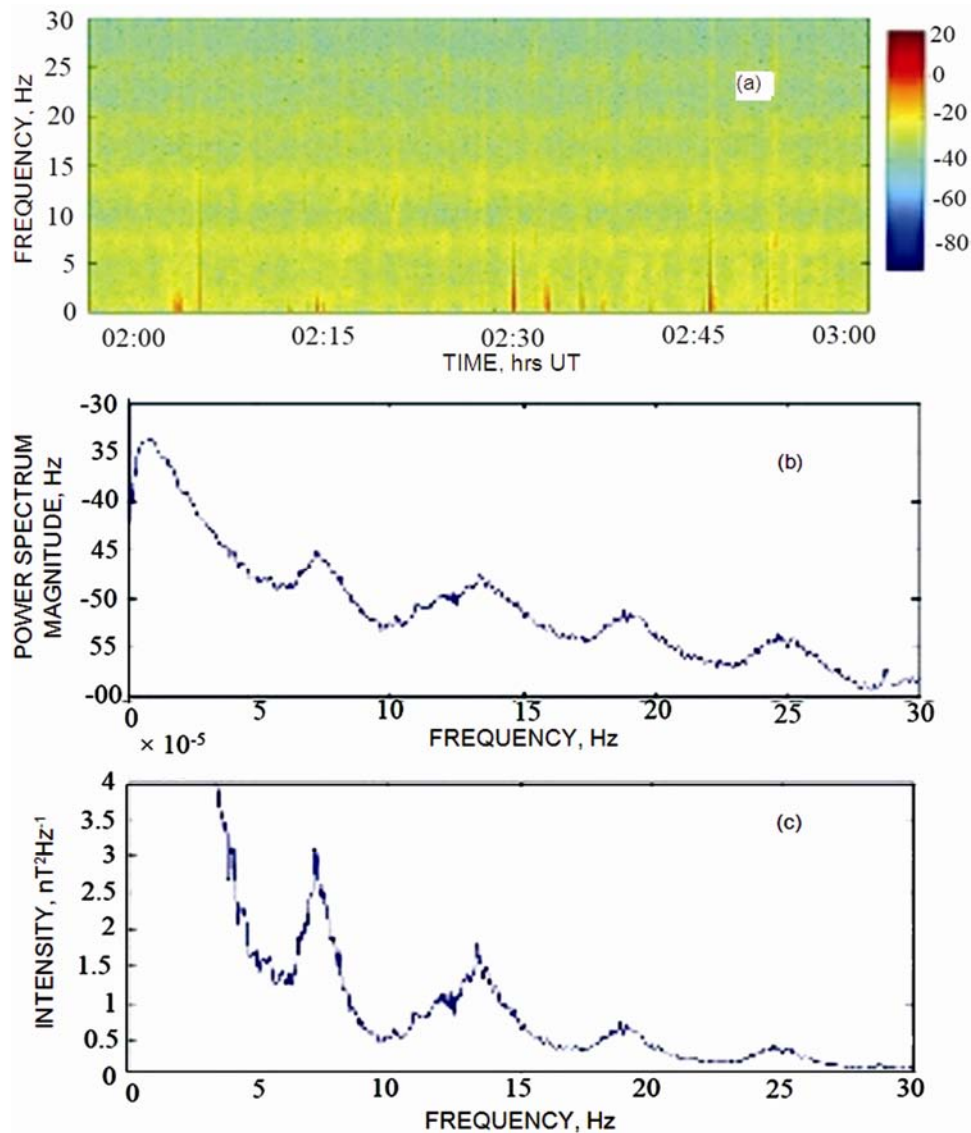
Fig. 1 — (a) Frequency-time spectrogram of the ELF/ULF data recorded on 18 February 2012 at Agra showing four Schumann resonance (SR) bands; (b) Variation of power spectral density (PSD) of the data; and (c) corresponding intensity-frequency variation

3 Results and Discussion

3.1 Global distribution of thunderstorm activities

Since the intensity of the first mode is positively correlated with the intensity of the thunderstorms[17], the diurnal variation of the first mode is studied for the three seasons, viz. summer (May-August), winter (November-February) and two equinoxes combined together (March-April and September-October) as done by Tyagi *et al.*[13] but for the period 01 March 2011 - 29 February 2012. However, in the present study, the intensity records are considered for each day and the integrated intensity of first three modes is calculated because a model SR intensity depends not only on the activities of the sources but also on the source-observer geometries. The consideration of integrated intensity may effectively neutralize the geometrical factors. From a general scanning of the data, it is found that the intensities of the second and third modes constitute approximately 40 percent of the total intensity of the three modes.

In Fig. 2(a), the diurnal variation of SR intensities is shown for the three seasons deduced from X and Y components of data observed at Agra station. Here, it is found that X-component data show larger intensity than Y-component for the simple reason that the nearest thunderstorm source in south-east Asia lies to the east of Agra station. Further, the curves in this figure show more distinct peaks and render more

information than those in Tyagi *et al.*[13], possibly due to modification in data processing. The intensity variation shows distinct peaks at 0600, 1000 and 1900 hrs UT corresponding to the three sources in south-east Asia, Africa, and America as found in Tyagi *et al.*[13]. The African source indicates two peaks possibly due to north-south movement of the thunderstorms in the broad noon period of Africa[3]. Similar variations may be seen also from the Y-component data for equinoxes and winter but a broad peak appears in summer.

In Fig. 2(b), the monthly variation of the SR intensity duly compared with OTD data is shown as is done Tyagi *et al.*[13] However, in the present study, it is found that the peak thunderstorm activity lies in the month of August, whereas in the previous study of 2007 (pre-SCM period), it occurred in the month of July. A possible reason for the shift in the peak thunderstorm activities may be given in view of increasing solar cycle period during which enhanced number of solar flares occur (as shown in Fig. 3), which deflect the galactic cosmic rays away from reaching towards the ground such that cloud formation and movement are delayed[18].

3.2 Solar cycle effect on the first mode SR frequency

Ondraskova *et al*[11,19] have reported extraordinary fall in the first mode SR frequency observed at Modra observatory in Slovakia and attributed this to the following solar cycle period with a minimum during 2008-2009. They interpreted this result in terms of that given by Satori *et al.*[20] according to which changes in X-ray radiation dominates the variation in conductivity profile within the upper characteristic layer (90-100 km) of E-region and the decrease of the conductivity by up to one order of magnitude over the solar cycle is responsible for the decrease of the SR frequency to several tenths of Hz.

In Fig. 3(a), the monthly variation of average first mode frequency is shown for the period under consideration (01 March 2011 - 29 February 2012), which was an increasing period of current solar cycle (2009-2020). In Fig. 3(b), the variation of number of M and X classes of solar flares is shown by histograms in which open portion shows the number of X-class and crossed portion shows the same for M class. The variation in number of solar flares shows clearly a decreasing trend from 2006 to 2009 (no flare occurred in 2009) and a rapid increase
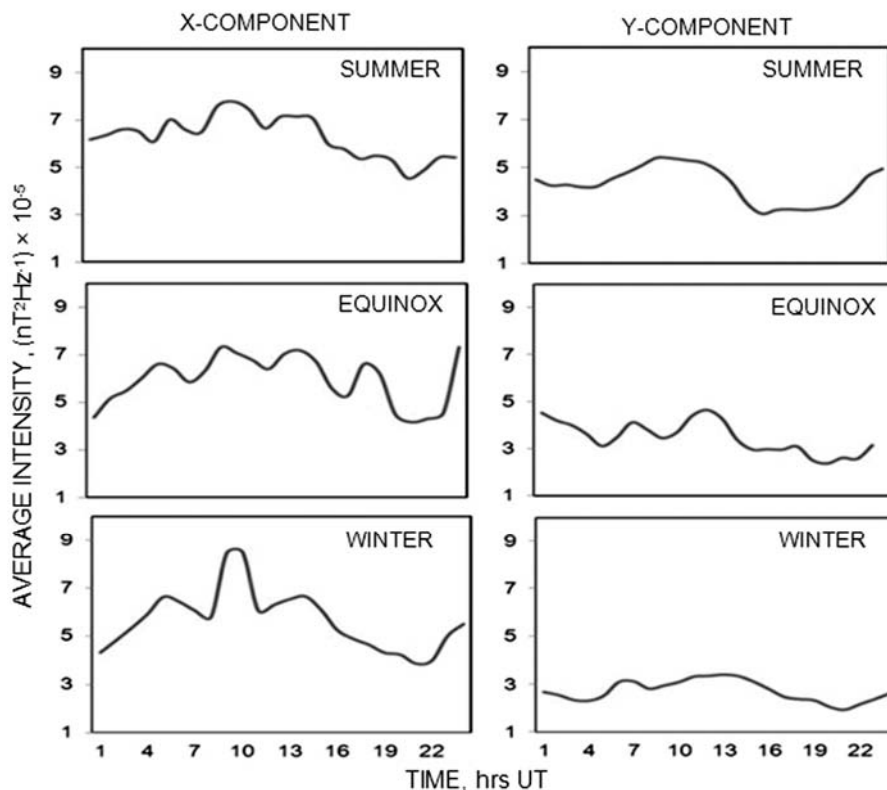
Fig. 2(a) — Diurnal variation of intensity of SR of X and Y-components during summer, equinoxes and winter months deduced from integrated intensities of first three modes
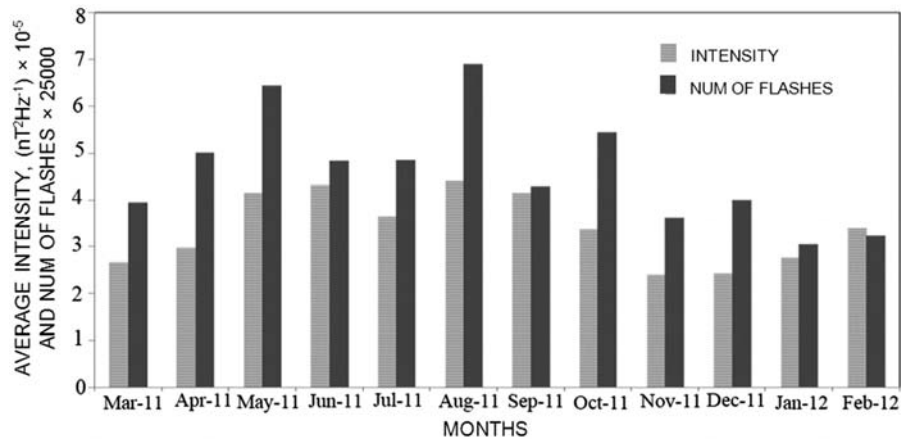
Fig. 2(b) — Monthly variation of global thunderstorm activities and a comparison with OTD data obtained from Lightning Image Sensor (LIS) on the satellite
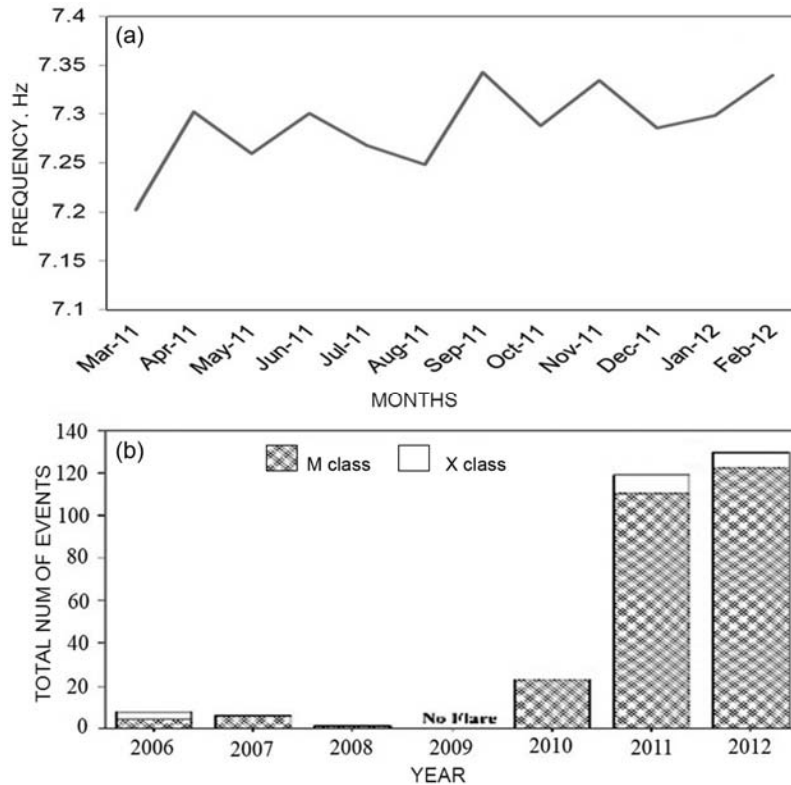
Fig. 3— (a) Monthly average variation of first mode SR frequency (X-component) (b) Variation of number of M and X classes of solar flares occurred between the years 2006 and 2012

onwards. The increasing trend in the first mode SR frequency in Fig. 3(a) may be explained clearly in the light of increasing effect of solar flares which increases the conductivity in the lower region of the ionosphere. The present results provide a convincing support to earlier workers[11,19,20] who attributed the decrease in first mode SR frequency to decreasing solar cycle effect.

3.3 Interpretation of diurnal variation of first mode SR frequency in terms of source-observer distance

Tyagi et al.[13] have discussed the diurnal variation in first mode frequency in terms of source-observer distance and ionospheric effect in detail. In order to examine the effect of increasing solar cycle period, the same calculations is repeated for the period under consideration and the results of diurnal variation

are presented for the three seasons, viz. summer (May-August), winter (November-February) and two equinoxes combined together (March-April, September-October) in the top three panels of Fig. 4. It is found that the graphical variations obtained show more closeness to those of Satori[21]. Some differences in the variation of the present results as compared to that of Satori[21] may be attributed to location of the observing station.

As suggested by Satori[21], the diurnal variation in the first mode SR frequency is due to North-South migration of global thunderstorm activities and it is proportional to source-observer distance. In order to verify this, the variation of source-observer distance (SOD) is shown in the bottom panel of Fig. 4, which are calculated by considering the relation (4.56) of Nickolaenko & Hayakawa[3] and assuming the observer

located at Agra (co-latitude 63°N, longitude 78°E), and a mid-day (1200 hrs UT) source (thunderstorm) at the equator (co-latitude 90°N). The present results show that as the time goes by, the distance between the source and observer varies modifying the SR mode amplitude. It may be seen from Fig. 4 that the diurnal variation of peak frequency of the first mode for summer and equinoxes look similar to that of calculated source-observer distance (SOD) presented in the bottom panel of Fig. 4 to a great extent.

3.4 Size of the thunderstorm region (effective lightning areas)

In the last Fig. 5, the variation of frequency range dF_1 is shown, which is the maximum daily value minus the minimum daily value of the first SR mode frequency ($dF_1 = f_1^{max} - f_1^{min}$). This parameter has been used to establish effective size zone
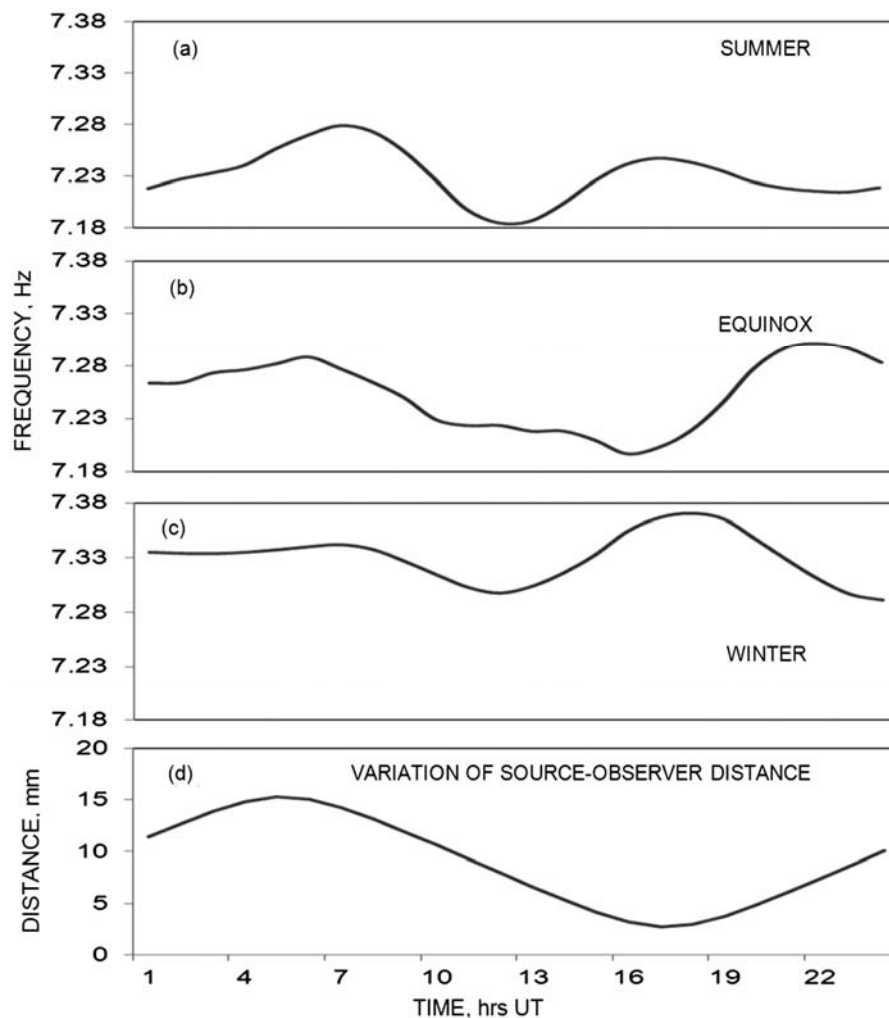
Fig. 4 — (a)-(c) Diurnal variation of average first mode SR frequency during the three seasons of summer, equinoxes, and winter; and (d) Variation of source-observer distance deduced theoretically
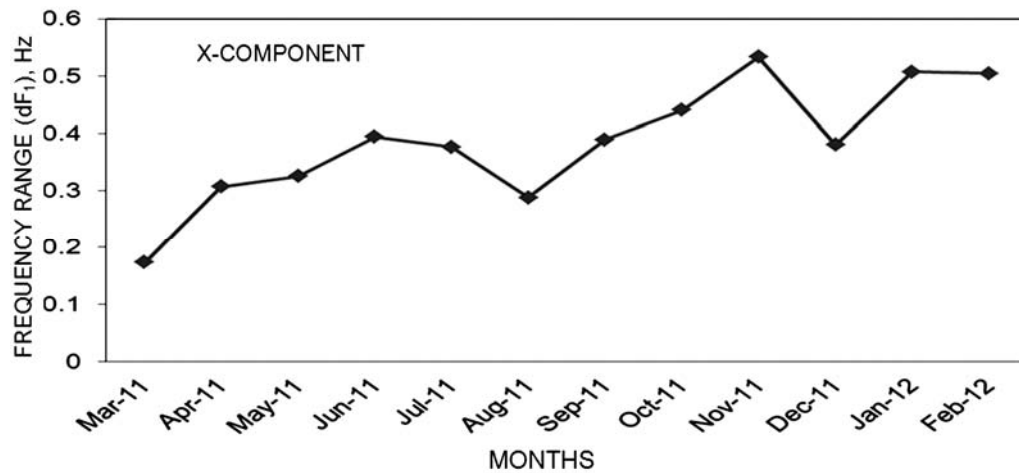
Fig. 5 — Monthly variation of frequency range dF_1 [two drops in the months of August and December corresponding to effective lightning activities are seen clearly]

occupied by the world wide thunderstorm activity from the SR records. In fact, the size zone is assumed to be in a circular area with source diameter in hours moving along the equatorial region[22,23]. The frequency range dF_1 varies inversely with the size of the thunderstorm region[11,22].

Two observations are made from the variation of dF_1 in Fig. 5: (i) the curve increases as the month increases, and (ii) there are two distinct drops in dF_1, one in the month of August 2011, and other in December 2011. While the increasing trend is due to increasing solar cycle period, the two drops are indicatives of intense thunderstorm activities in the respective two months. The first drop corresponding to a decreasing frequency range from the month of June, which increases up to September and is a wider one than the other drop in which the frequency decrease is limited between November 2011 and January 2012. Incidentally, these two thunderstorm zones coincide with the rainy seasons in India. The one around August has already been verified by the OTD data in Fig. 2(b).

Nickolaenko & Hayakawa[3] and Ondraskova et al.[19] have suggested a method to determine the calibration curves from which source diameters in hours may be determined corresponding to changes in dF_1. These source diameters may be converted into longitudinal range (source width) of the thunderstorm regions.

Although, the SR data show the variation of global thunderstorm activity and one needs to separate the local effect from the global one as suggested earlier[12]; here, since Agra observing station is

close to the center of second major South-East Asian source (around 3000 km), which lies in Indonesia, it is assumed conveniently that the present data corresponds largely to local variations. Further, the determinations of effective lightning areas from SR data are usually done by measuring the vertical component of SR electric field[3,19] rather than horizontal component of magnetic field. However, accuracy in the result depends more on the processing technique[19,20]. Since, there is no electric field measurement system at the Agra station, it is considered that the processing method employed in the present study may render accuracy in the result even by employing the measurement of horizontal components of the SR data.

4 Conclusion

A system of 3-component search coil magnetometer is employed and Schumann resonance phenomenon is monitored at a low latitude station Agra in India. The data for a period of one year, between 01 March 2011 and 29 February 2012, which corresponds to the post period of SCM of 2008-2009 are analysed and the results are compared with those obtained during a previous study during 01 April 2007 - 31 March 2008, which correspond to pre-period of SCM of 2008-2009. It is found that there are significant shifts in the period of global thunderstorm activities from the month of July to August in the two periods. It is also indicated from the variation of frequency range dF_1 in post period that the effective lightning areas in summer and winter months lie around August and December in Indian

region. Finally, it is shown theoretically how the variation in first mode SR frequency is related to source-observer distance.

Acknowledgement

References

1   Schumann W O, On the free oscillations of a conducting sphere which is surrounded by an air layer and an ionosphere shell, *Z Nat.forsch (Germany)*, 7a (1952) pp 149-154 (in German).

2   Balser M & Wagner C A, Observation of Earth-ionosphere cavity resonances, *Nature (UK)*, 188 (1960) pp 638-641.

3   Nickolaenko A P & Hayakawa M, *Resonances in the earth-ionosphere cavity* (Kluwer Academic Publishers, Dordrecht, the Netherlands), 2002.

4   Price C & Melnikov A, Diurnal, seasonal and inter-annual variations of the Schumann resonance parameters, *J Atmos Sol-Terr Phys (UK)*, 66 (2004) pp 1179-1185.

5   Melnikov A, Price C & Satori G, Influence of solar terminator passages on Schumann resonance parameters, *J Atmos Sol-Terr Phys (UK)*, 66 (2004) pp 1187-1194.

6   Pechony O, Price C & Nickolaenko A P, Relative importance of the day-night asymmetry in Schumann resonance amplitude records, *Radio Sci (USA)*, 42 (2007) doi: 10.1029/2006RS003456.

7   Greenberg E & Price C, Diurnal variation of ELF transients and background noise in the Schumann resonance band, *Radio Sci (USA)*, 42 (2007) RS2S08, doi: 10.1029/2006RS003477.

8   Hayakawa M, Ohta K, Nickolaenko A P & Ando Y, Anomalous effect in Schumann resonance phenomena observed in Japan possibly associated with the Chi-Chi earthquake in Taiwan, *Ann Geophys (Germany)*, 23 (2005) pp 1335-1346.

9   Williams E R & Satori G, Solar radiation- induced changes in ionospheric height and the Schumann resonance waveguide on different timescales, *Radio Sci (USA)*, 42 (2007) RS2S11, doi: 10.1029/2006RS003494.

10 De S S, De B K, Sarkar B K, Bandyopadhyay B, Haldar D K, Paul S & Barui S, Analyses of Schumann resonance spectra from Kolkata and their possible interpretations, *Indian J Radio Space Phys*, 38 (2009) pp 208-214.

11 Ondraskova A, Sevcik S & Kostecky P, A significant decrease of the fundamental Schumann resonance frequency during the solar cycle minimum of 2008-9 as observed at Modra Observatory, *Contrib Geophys Geod (Slovakia)*, 39 (4) (2009) pp 345-354.

12 Nickolaenko A P, Yatsevich E I, Shvets A V, Hayakawa M & Hobara Y, Universal and local time variations deduced from simultaneous Schumann resonance records at three widely separated observatories, *Radio Sci (USA)*, 46 (5) (2011), doi: 10.1029/2011RS004663.

13 Tyagi R, Singh B, Singh O P & Dua R L, Characteristics of global thunderstorm extracted from Schumann Resonance at Agra, *J Adv Res Elecr Electron Instrum Eng (India)*, 2 (2013) pp 1129-1137.

14 Singh B, Tyagi R, Hobara Y & Hayakawa M., X-rays and solar proton event induced changes in the first mode Schumann resonance frequency observed at a low latitude station Agra, India, *J Atmos Sol-Terr Phys (UK)*, 113C (2014) pp 1-9, doi: 10.1016/j.jstp.2014.02010.

15 Welch P D, The use of Fast Faurier transform for the estimation of power spectra: A method passed on time averaging over short modified periodgrams, *IEEE Trans Audio Electroacoust (USA)*, AU-16 (1967) pp 70-73.

16 Bingham C, Godfrey M D & Turkey J W, Modern techniques of power spectrum estimation, *IEEE Trans Audio Electroacoust (USA)*, AU-15 (1967) pp 56-66.

17 Williams E R, The Schumann resonance: a global tropical thermometer, *Science (USA)*, 256 (1992) pp 1184-1187.

18 Lakshmi D R, A brief review of solar activity modulations of global electric circuit, in *Proceedings of DST sponsored workshop on Electrodynamical coupling of atmospheric regions* (Indian Institute of Geomagnetism, Navi Mumbai), 2008, pp 25-26.

19 Ondraskova A, Sevcik S & Kostecky P, Decrease of Schumann resonance frequencies and changes in the effective lightening areas towards the solar cycle minimum of 2008-2009, *J Atmos Sol-Terr Phys (UK)*, 73 (2011) pp 534-543.

20 Satori G, Williams E & Mushtak V, Response of the Earth-ionosphere cavity resonator to the 11-year solar cycle in X-radiation, *J Atmos Sol-Terr Phys (UK)*, 67 (2005) pp 553-562.

21 Satori G, On the dynamics of the north-south seasonal migration of global lightning, *Proc of 12th International Conference on Atmospheric Electricity: Global Lightning and Climate* (Versailles, France), 2003, pp 1-4.

22 Nickolaenko A P & Rabinowicz L M, Study of annual changes of global lightning distribution and frequency variations of the first Schumann resonance mode, *J Atmos Sol-Terr Phys (UK)*, 57 (1995) pp 1345-1348.

23 Nickolaenko A P, Satori G, Ziegler V, Rabinowicz L M & Kudintseva I G, Parameters of global thunderstorm activity deduced from the long-term Schumann resonance records, *J Atmos Sol-Terr Phys (UK)*, 60 (1998) pp 387-399.